RESEARCH REPORTS
Biomaterials & Bioengineering

N. Chosa[1*†], M. Taira[2†], S. Saitoh[2], N. Sato[1], and Y. Araki[2]

Departments of [1]Biochemistry and [2]Dental Materials Science and Technology, Iwate Medical University School of Dentistry, Morioka, Iwate, 020-8505 Japan; [†]authors contributing equally to this work; *corresponding author, nchosa@iwate-med.ac.jp

J Dent Res 83(6):465-469, 2004

Characterization of Apatite Formed on Alkaline-heat-treated Ti

ABSTRACT

Alkaline-heat-treated titanium self-forms an apatite surface layer *in vivo*. The aim of the present study was to materialistically characterize the surface of alkaline-heat-treated titanium immersed in simulated body fluid (AHS-TI) and to examine the differentiation behavior of osteoblasts on AHS-TI. SEM, thin-film XRD, FTIR, and XPS analyses revealed that AHS-TI contained a 1.0-μm-thick, low-crystalline, and [002] direction-oriented carbonate apatite surface. Human osteoblast-like SaOS-2 cells were cultured on polystyrene, titanium, and AHS-TI, and RT-PCR analyses of osteogenic differentiation-related mRNAs were conducted. On AHS-TI, the expression of bone sialoprotein mRNA was up-regulated as compared with that on polystyrene and titanium ($p < 0.05$). On AHS-TI, the expression of osteopontin and osteocalcin mRNAs was up-regulated as compared with that on polystyrene ($p<0.05$). The results indicate that the apatite was bone-like and accelerated the osteogenic differentiation of SaOS-2, suggesting that alkaline-heat treatment might facilitate better integration of titanium implants with bone.

KEY WORDS: apatite, titanium, alkaline-heat treatment, osteoblasts, RT-PCR.

Received April 30, 2003; Last revision March 29, 2004; Accepted March 30, 2004

A supplemental appendix to this article is published electronically only at http://www.dentalresearch.org.

INTRODUCTION

Titanium has been widely used in endosseous dental implants. Alkaline-heat treatment is a simple and cost-effective method of coating titanium with apatite (Kokubo *et al.*, 1996). It has been reported that NaOH treatment of pure titanium causes a sodium titanate hydrogel surface layer to form. Subsequent heat treatment at 600°C results in an amorphous sodium titanate surface layer. When immersed in simulated body fluid or placed *in vivo*, alkali-heat-treated titanium forms an apatite surface layer (coded as AHS-Ti) (Kokubo *et al.*, 1996). There have been few reports, however, which scrutinized this apatite coating (Takadama *et al.*, 2001). The apatite layer was reported to be both osteo-conductive and -inductive, which is advantageous for the clinical usage of titanium implants (Yan *et al.*, 1997). Furthermore, there have been few attempts to examine, systematically, the osteogenic differentiation of human osteoblasts cultured on apatite itself (Massas *et al.*, 1993; Nishio *et al.*, 2000).

We hypothesized that an apatite layer did exist on AHS-TI in a form analogous to natural bone and thus could accelerate the osteogenic differentiation of osteoblasts. In this study, therefore, we first characterized the surface structure of alkali-heat-treated titanium analytically before and after soaking it in SBF. Then, on the apatite layer (AHS-TI) as well as polystyrene culture dishes and titanium, we cultured human osteoblast-like cells, SaOS-2, and examined the expression of 6 osteogenic differentiation-related marker mRNAs by RT-PCR up to 4 wks after confluence. The osteogenic differentiation proceeds sequentially with the appearance of specific osteogenic marker mRNAs. Usually, alkaline phosphatase (ALP), type I collagen (COL), and osteonectin (OSN) mRNAs are expressed first, followed by osteopontin (OPN) and bone sialoprotein (BSP) mRNAs, while osteocalcin (OSC) mRNA emerges last (Beck *et al.*, 2000). The expression of these mRNAs on AHS-TI needed to be clarified.

MATERIALS & METHODS

Alkali-heat Treatment of Ti

Commercially pure (c.p.) Ti plates (10 x 10 x 1 mm for surface analyses and 25 x 25 x 1 mm for cell culture) (Ti > 99.8%, Kobe Steel, Kobe, Japan) were mechanically polished with 100-, 180-, and 320-grit sand paper, successively, and ultrasonically washed in acetone and distilled water. The polished titanium plates (TI) were then soaked in a 5M NaOH solution at 60°C for 24 hrs, followed by gentle washing in distilled water and drying in an oven at 37°C for 24 hrs (A-TI). A-TI plates were subsequently heated to 600°C at a rate of 5°C/min in an electrical furnace, kept at 600°C for 1 hr, and allowed to cool in the furnace (AH-TI).

Soaking in Simulated Body Fluid

The AH-TI plates were dipped at 37°C in 50 mL of simulated body fluid (SBF) with a pH of 7.4 and ionic concentrations (142.0 mM Na^+, 5.0 mM K^+, 1.5 mM

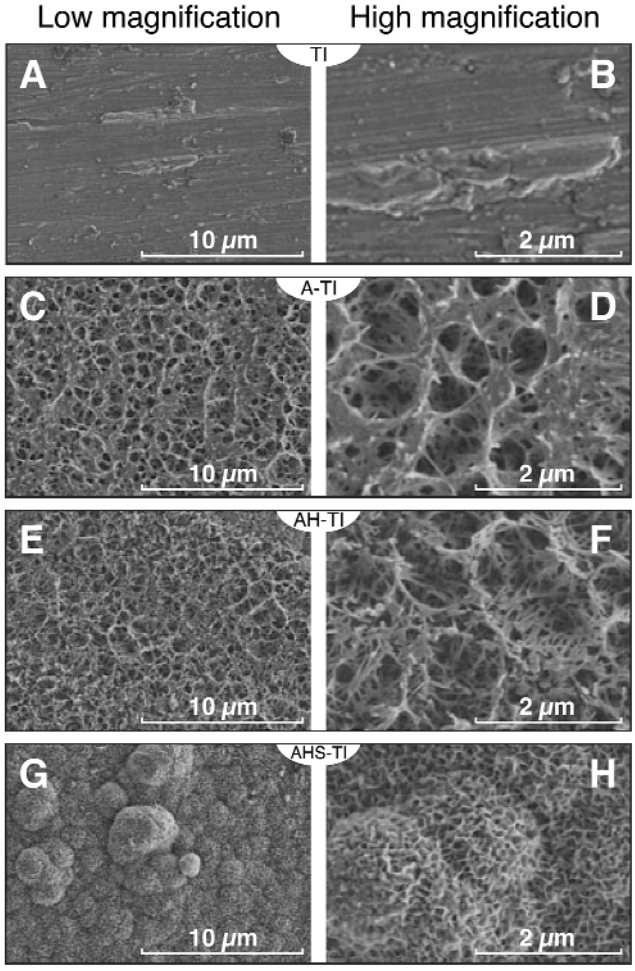

Figure 1. Surface image of AHS-TI. SEM photo-micrographs at low (left) and high (right) magnification of **(A,B)** TI (polished titanium), **(C,D)** A-TI (alkali-treated titanium), **(E,F)** AH-TI (alkali-heat-treated titanium), and **(G,H)** AHS-TI (alkali-heat-treated titanium soaked in SBF) (n = 1). Note: TI had a rough scratched surface, both A-TI and AH-TI had porous honeycomb structures, and AHS-TI had a domed structure.

Mg^{2+}, 2.5 mM Ca^{2+}, 147.8 mM Cl^-, 4.2 mM HCO_3^-, 1.0 mM HPO_4^{2-}, and 0.5 mM SO_4^{2-}) resembling those of human blood plasma (Kokubo *et al.*, 1996). We prepared the SBF by dissolving reagent-grade NaCl, $NaHCO_3$, KCl, $K_2HPO_4 \cdot 3H_2O$, $MgCl_2 \cdot 6H_2O$, $CaCl_2$, and Na_2SO_4 in distilled water, and buffered it at pH 7.4 with tris-hydroxymethyl aminomethane [$(CH_2OH)_3CNH_2$] and hydrochloric acid at 37°C. The SBF solution was replaced every two days. After soaking for 8 days, the plates were washed with distilled water, and dried on a clean bench (AHS-TI).

Surface Analyses

The surfaces of TI, A-TI, AH-TI, and AHS-TI were examined by scanning electron microscopy (SEM) (S-700, Hitachi, Tokyo, Japan), thin-film x-ray diffraction (XRD) (JDX-3500, JEOL, Tokyo, Japan), Fourier transform infrared spectroscopy (FTIR) (Spectrum One, Perkin Elmer Japan, Kanagawa, Japan), and x-ray photoelectron spectroscopy (XPS) (AXIS-HSi, Kratos, Manchester, UK). In the thin-film XRD measurements, Cu-Kα radiation was used as an x-ray source. The glancing angle of the specimen (θ angle) was fixed at 1° against the incident beam. The characteristic XRD peaks were labeled with reference to standard powder diffraction data (JCPDS, 1991). In the XPS measurements, Al-Kα radiation was used as an x-ray source. The XPS take-off angle was set at 90°. Following XPS wide scans, XPS narrow scans of O 1s, Ti 2p, Ca 2p, P 2p, and Na 1s regions were conducted for the quantification of atomic compositions. The depth profile was taken on AHS-TI.

Cell Culture

Human osteoblast SaOS-2 cells were cultured in Eagle's α-modified minimum essential medium (Sigma, St. Louis, MO, USA) supplemented with 10% fetal bovine serum (Gibco BRL, Rockville, MD, USA). The cells (5×10^5) were plated in polystyrene culture dishes (PS) (#150288, Nalge Nunc International, Tokyo, Japan), or on TI plates in PS and on AHS-TI plates in PS and cultured. Every 3 days, the medium was exchanged, and TI and AHS-TI plates were transferred to new PS so that the spreading of the cells from the plates to PS could be minimized. After confluence (dated at 0 wk), the cells were further cultured for 1, 2, 3, or 4 wks.

RT-PCR

Total RNA of the cells cultured on PS, TI, or AHS-TI was isolated with ISOGEN reagent (Nippongene, Tokyo, Japan), and the cDNA was synthesized by TrueScript II (Sawady Technology, Tokyo, Japan) according to the manufacturer's instructions. PCR was performed with the following primers: alkaline phosphatase (ALP, 5′-CTCGTTGACACCTGGAAGAGC-3′ and 5′-ACAGGATGG CAGTGAAGGGCT-3′); type-I collagen (COL, 5′-ACTGGGG AAACCTGTATCCGG-3′ and 5′-AAGGGCAGGCGTGAT GGCTTA-3′); osteonectin (OSN, 5′-CCGAAGAGGAGGTGG TGGCGG-3′ and 5′-ACGGGGTGGTCTCCTGCCTCC-3′); osteopontin (OPN, 5′-CCTAGCCCCACAGACCCTTCC-3′ and 5′-CTGTCCTTCCCACGGCTGTCC-3′); bone sialoprotein (BSP, 5′-CAACACTGGGCTATGGAGAGGACGC-3′ and 5′-GTAATTGTCCCCACGAGGTTCCCCG-3′); osteocalcin (OSC, 5′-CAGCAAAGGTGCAGCCTTTGT-3′ and 5′-TCCTGAAA GCCGATGTGGTC-3′); glyceraldehyde-3-phosphate dehydrogenase (GAPDH, 5′-TGGTATCGTGGAAGGACTCATG-3′ and 5′-TCTCTTCCTCTTGAGCTCTTGC-3′). PCR cycle conditions were 95°C for 30 sec, 60°C for 60 sec, and 72°C for 90 sec for 20, 22, or 24 cycles. The relative expression levels of each mRNA were determined by their densitometric value divided by that of the corresponding GAPDH control, with the use of NIH Image (National Institutes of Health, Bethesda, MD, USA).

Statistics

Data were presented as the mean ± standard deviation (SD). Statistical analysis was performed with the Student *t* test, and p-values < 0.05 were considered 'significant'.

RESULTS

Surface Characterization

It became evident from SEM photo-micrographs (Fig. 1), thin-film XRD (Fig. 2A), FTIR (Fig. 2B), XPS wide-scan spectra (Figs. 3A-D), and the depth profile of AHS-TI (Fig. 3E) that AHS-TI had (a) a domed carbonate-apatite surface layer which was about 1.0 μm thick, low-crystalline, and preferentially oriented in the [002] direction with (b) a first graded zone, (c) a Ti-O layer, (d) a second graded zone, and (e) a titanium base.

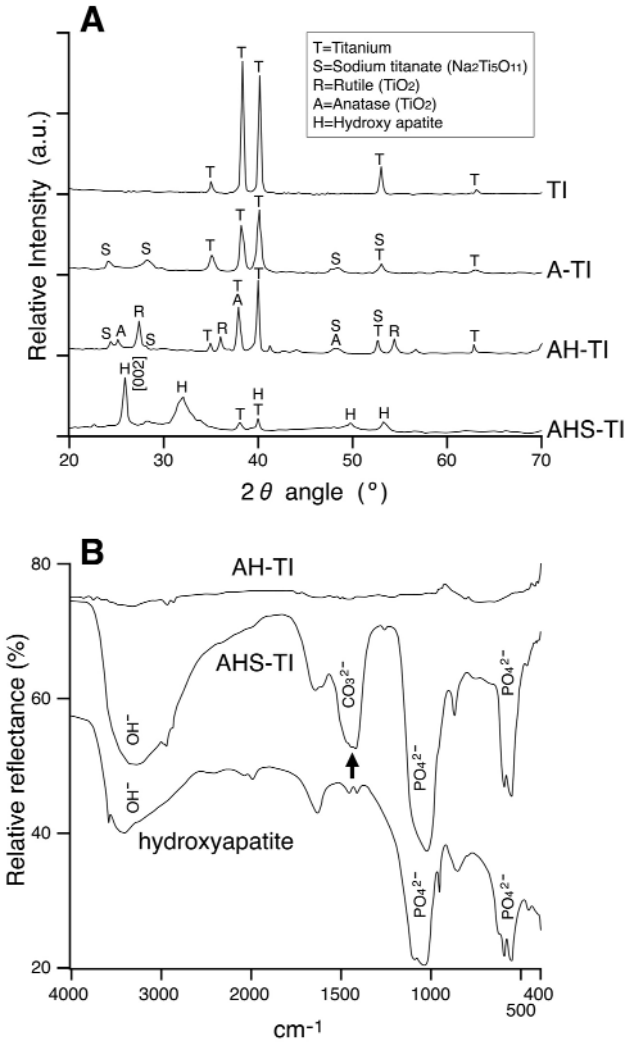

Figure 2. AHS produced carbonate-apatite on TI. **(A)** Thin-film XRD profiles of TI (polished titanium), A-TI (alkali-treated titanium), AH-TI (alkali-heat-treated titanium), and AHS-TI (alkali-heat-treated titanium soaked in SBF) (n = 1). Note: TI had 5 metallic titanium peaks; A-TI had peaks of amorphous sodium titanate and titanium; AH-TI had peaks of rutile, sodium titanate, and titanium; and AHS-TI had peaks of hydroxyapatite along with peaks of trace titanium. **(B)** FTIR charts of AH-TI, AHS-TI, and hydroxyapatite (n = 1). Note: Arrow indicates existence of CO_3^{2-} in AHS-TI.

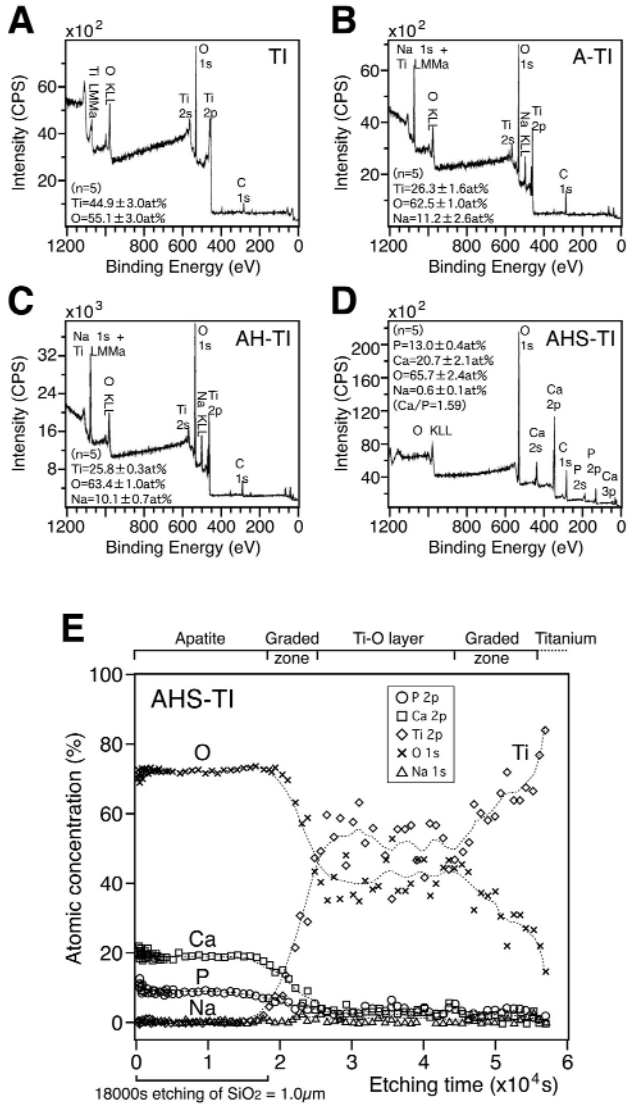

Figure 3. AHS-TI consisted of 1.0 μm carbonate-apatite and underlying layered structures. XPS wide-scan spectra of the surfaces of **(A)** TI (polished titanium), **(B)** A-TI (alkali-treated titanium), **(C)** AH-TI (alkali-heat-treated titanium), and **(D)** AHS-TI (alkali-heat-treated titanium soaked in SBF) (representative case). Note: The chemical composition (at%) of each element is also depicted (mean ± SD, n = 5). **(E)** The depth profile of AHS-TI (n = 1). Note: AHS-TI consisted of 5 distinctive layers. From the surface, the apatite layer continued with a thickness of about 1.0 μm. Below the first graded zone, there is a Ti-O layer presumably consisting of titanium and TiO_2 oxide about 1.0 μm thick. Below the second graded zone, there is base metallic titanium.

Osteogenic Differentiation

Expression levels of ALP and COL mRNAs on TI and AHS-TI declined as the culture period increased to more than 3 wks, while that on PS remained *quasi*-constant. Expression levels of OSN mRNA were kept constant on the 3 materials examined (Fig. 4A). Expression levels of OPN mRNA were significantly higher on AHS-TI than on PS and TI at 3 and 4 wks ($p < 0.05$), although the former levels were not different from those on TI at 2 wks. The expression of BSP mRNA on AHS-TI was induced at 1 wk, and overwhelmed that on PS and TI in all 4 culture periods ($p < 0.05$). The expression of OSC mRNA on AHS-TI appeared after 2 wks, but its magnitude gradually declined at 3 and 4 wks, being greater than that of PS after 2 wks ($p < 0.05$) (Fig. 4B). [Supplemental material can be found in the APPENDIX.]

DISCUSSION

Our structural findings of AHS-TI were basically consistent with those reported previously (Takadama *et al.*, 2001). Our new findings were that the apatite was oriented in the [002] direction, contained CO_3^{2-}, and possessed complicated layered structures beneath the surface. The domed structure of the

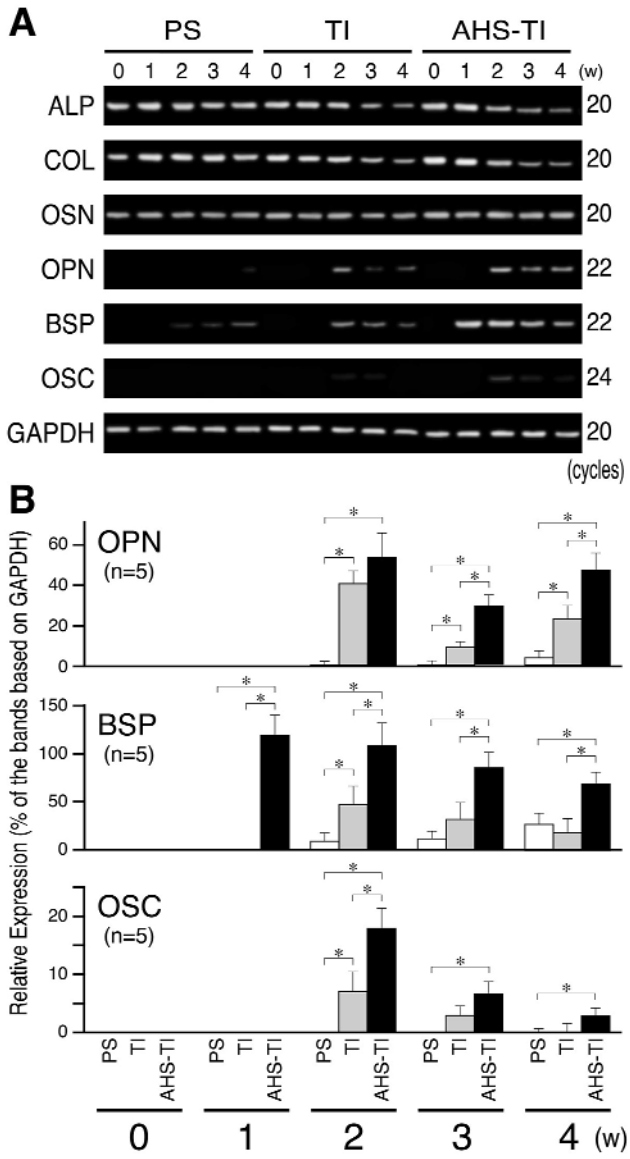

Figure 4. On AHS-TI, the expression of early-stage differentiation-related mRNAs was down-regulated and that of middle- to late-stage differentiation-related mRNAs was up-regulated. **(A)** The changes in the levels of expression of 6 osteogenic differentiation marker mRNAs and GAPDH of SaOS-2 cultured for 1, 2, 3, or 4 wks on PS (polystyrene dish), TI (polished titanium), and AHS-TI (alkali-heat-treated titanium soaked in SBF) (representative case). **(B)** The relative expression levels of OPN, BSP, and OSC on PS, TI, and AHS-TI (mean ± SD, n = 5). *$p < 0.05$. Note: AHS-TI accelerated the osteogenic differentiation of SaOS-2 cells with ALP and COL mRNAs down-regulated and OPN, BSP, and OSC mRNAs up-regulated.

apatite appeared to consist of many needle-shaped crystals, along the length of which columnar Ca might line up. The carbonate apatite identified here was analogous to the inorganic phase of human bones (Bigi *et al.*, 1997). Its composition and structure are regarded as more suitable for osseous implants than those of hydroxyapatite (Hasegawa *et al.*, 2003). The apatite structure of AHS-TI may differ from that precipitated with other methods (Massaro *et al.*, 2001).

Our results clarified that AHS-TI accelerated osteogenic differentiation in that the expression of early-stage differentiation-related mRNAs was down-regulated and that of middle- to late-stage differentiation-related mRNAs was up-regulated, compared with the results for PS and TI. This might be attributed to the early settling of SaOS-2 on apatite. On apatite, the cells started proliferating earlier, but their motility ceased earlier, leading to earlier osteogenic differentiation (Okamura *et al.*, 2001). Another reason might stem from the existence of phosphate on the apatite surface, which might up-regulate the production of OPN (Beck *et al.*, 2000). Other factors, such as up-regulation of osteoblast-specific transcription factor Cbfa1, might be involved, but this is beyond the scope of this study. The expression of BSP mRNAs best clarified the change in osteogenic differentiation, and is considered a more reliable indicator of osteogenic differentiation of osteoblasts than often-unstable OSC mRNAs (Cooper *et al.*, 2001). TI might contain traces of calcium-phosphate precipitates after immersion in SBF (Hanawa and Ota, 1991), and thus, could slightly accelerate the osteogenic differentiation. It appeared that PS alone little accelerated the osteogenic differentiation but had an important role in improving cell adhesion. The use of SaOS-2 seemed reasonable to examine the material's influence on osteogenic differentiation.

Referring to c.p. endosseous titanium implants, alkaline-heat treatment would be beneficial because it can improve the osteo-integration of implants with bone through the apatite layer.

ACKNOWLEDGMENTS

The study was supported by (1) a Grant-in-Aid for High-performance Biomedical Materials Research, (2) a Grant-in-Aid for the Open Research Project from the Ministry of Education Culture, Sports, Science and Technology, Japan, and (3) CREST of JST (Japan Science and Technology Corporation).

REFERENCES

Beck GB Jr, Zerler B, Moran E (2000). Phosphate is a specific signal for induction of osteopontin gene expression. *Proc Natl Acad Sci USA* 97:8352-8357.

Bigi A, Cojazzi G, Panzavolta S, Ripamonti A, Roveri N, Romanello M, *et al.* (1997). Chemical and structural characterization of the mineral phase from cortical and trabecular bone. *J Inorg Biochem* 68:45-51.

Cooper LF, Harris CT, Bruder SP, Kowalski R, Kadiyala S (2001). Incipient analysis of mesenchymal stem-cell-derived osteogenesis. *J Dent Res* 80:314-320.

Hanawa T, Ota M (1991). Calcium phosphate naturally formed on titanium in electrolyte solution. *Biomaterials* 12:767-774.

Hasegawa M, Doi Y, Uchida A (2003). Cell-mediated bioresorption of sintered carbonate apatite in rabbits. *J Bone Joint Surg Br* 85:142-147.

JCPDS (Joint Committee on Power Diffraction Standards) (1991). Powder diffraction cards. Swarthmore, PA, USA.

Kokubo T, Miyaji F, Kim HM (1996). Spontaneous formation of bone-like apatite layer on chemically treated titanium metals. *J Am Ceram Soc* 79:1127-1129.

Massaro C, Baker MA, Cosentino F, Ramires PA, Klose S, Milella E (2001). Surface and biological evaluation of hydroxyapatite-based

coatings on titanium deposited by different techniques. *J Biomed Mater Res (Appl Biomater)* 58:651-657.

Massas R, Pitaru S, Weinreb MM (1993). The effects of titanium and hydroxyapatite on osteoblastic expression and proliferation in rat parietal bone cultures. *J Dent Res* 72:1005-1008.

Nishio K, Neo M, Akiyama H, Nishiguchi S, Kim HM, Kokubo T, *et al.* (2000). The effect of alkali- and heat-treated titanium and apatite-formed titanium on osteoblastic differentiation of bone marrow cells. *J Biomed Mater Res* 52:652-661.

Okamura A, Goto M, Goto T, Yoshinari M, Masuko S, Katsuki T, *et al.* (2001). Substrate affects the initial attachment and subsequent behavior of human osteoblastic cells (Saos-2). *Biomaterials* 22:2263-2271.

Takadama H, Kim HM, Kokubo T, Nakamura T (2001). An x-ray photoelectron spectroscopy study of the process of apatite formation on bioactive titanium metal. *J Biomed Mater Res* 55:185-193.

Yan WQ, Nakamura T, Kobayashi M, Kim HM, Miyaji F, Kokubo T (1997). Bonding of chemically treated titanium implants to bone. *J Biomed Mater Res* 37:267-275.

RESEARCH REPORTS
Biomaterials & Bioengineering

N. Chosa[1]*†, M. Taira[2]†, S. Saitoh[2], N. Sato[1], and Y. Araki[2]

Departments of [1]Biochemistry and [2]Dental Materials Science and Technology, Iwate Medical University School of Dentistry, Morioka, Iwate, 020-8505 Japan; †authors contributing equally to this work; *corresponding author, nchosa@iwate-med.ac.jp

Characterization of Apatite Formed on Alkaline-heat-treated Ti

J Dent Res 83(6):465-469, 2004

APPENDIX

This is 'supplemental material' that explains additional experimental results with Figs., emphasizes important findings obtained by this study, and refers to related studies conducted by other researchers with additional references.

(1) EDX Analysis and Related Matters

Energy-dispersed x-ray (EDX) (EMAX-7000, Horiba, Tokyo, Japan) analysis revealed that AHS-TI contained not only O, Na, P, Ca, and Ti but also minute amounts of Mg and Cl (Fig. 2C), implying that AHS-TI more resembled the inorganic phase of natural bone (Bigi *et al.*, 1997). XPS quantitative analyses of Mg and Cl were not carried out due to the low concentrations. XPS and XRD scanned the surface at a depth of about 10 nm and 1000 nm (1 μm), respectively. The element carbon could not be identified by EDX, because samples were sputtered with carbon for the chemical analyses of other elements, and were confirmed by FTIR. Cells might recognize the material on the uppermost surface that XPS could better identify. The scanned thickness of thin-film XRD was thought to be about 1 μm.

(2) Comments Concerning Massaro's Paper (2001) and Related Matters—3 Other Coating Methods *vs.* Alkaline-heat Treatment

Massaro *et al.* (2001) have used 3 different apatite coating techniques on titanium: (a) Plasma spray deposition brought about the thickest apatite layer, about 100 μm thick, which was least crystalline, lacked OH^-, and least affected the osteogenic differentiation of osteoblasts. (b) Sputter deposition produced the second thickest apatite layer, up to 10 μm in thickness, that was most crystalline, possessed abundant OH^-, and accelerated the osteogenic differentiation of osteoblasts. (c) Sol-gel coating formed the thinnest apatite+titania duplex layer, with a thickness less than 1 μm, which was third-best crystalline, possessed most OH^-, and increased the osteogenic differentiation of osteoblasts. Alkali-heat treatment examined here produced the second thinnest apatite layer which was oriented in the [002] direction (c-axis), possessed many OH^-, characteristically contained CO_3^{2-} in addition to minute amounts of Mg and Cl, and increased the differentiation of osteoblasts. Because the carbonate apatite is precipitated biomimetically and physiologically, which takes place *in vivo*, cell adhesion and cellular differentiation might take place efficiently on AHS-TI.

This biomimetic apatite coating method for titanium (*i.e.*, alkali-heat treatment) has heralded many related studies (Han *et al.*, 2001; Barrere *et al.*, 2002; Jonasova *et al.*, 2002; Lee *et al.*, 2002). It appeared that all apatite might accelerate the osteogenic differentiation of osteoblasts, more or less dependent upon the structure and composition of apatite layers.

For the apatite coating technique that increases the usefulness of commercially pure (c.p.) endosseous titanium implants, alkali-heat treatment might be the best choice, due to the ease of handling and low cost. Post-heat treatment (*i.e.,* at 400°C to 600°C) might increase the bond strength of the apatite coating with a titanium base (van Dijk *et al.*, 1996), which needs further consideration. Or, the intact thin carbonate-apatite layer on AHS-TI might be slowly bio-absorbed by macrophages and osteoclasts, etc., in the bone re-modeling system *in vivo* and be replaced in part by osseous ECM (extracellular matrix) that leads to a better integration of endosseous c.p. titanium implants with surrounding bone structures. Such aspects are not well-understood and need to be investigated as well.

(3) Mechanism of Apatite Coating on AH-TI by Immersion in SBF

Here, the suggested mechanism of apatite coating on AH-TI is quoted (Takadama *et al.*, 2001). When dipped in the body fluid

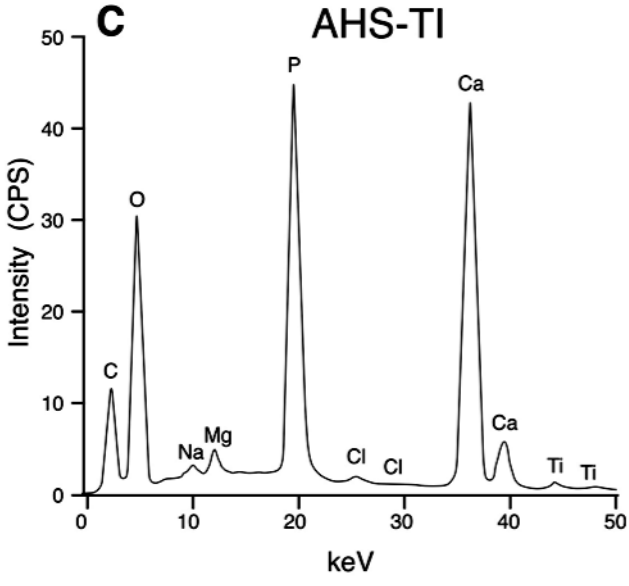

Figure 2. (C) AHS-TI further included Mg and Cl. EDX spectrum of AHS-TI and hydroxyapatite (n = 1). Note: Mg and Cl were included in addition to P, Ca, O, and Na. Ti came from base metallic titanium.

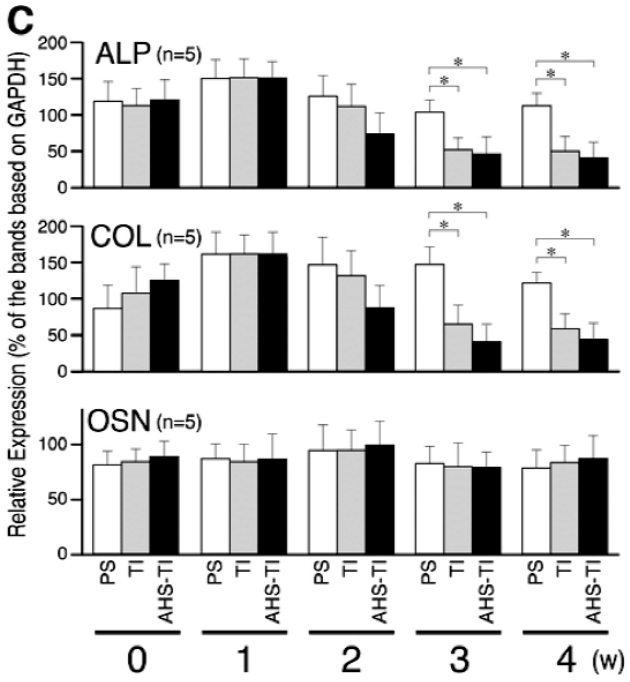

Figure 4. (C) AHS-TI and TI down-regulated ALP and COL. The relative expression levels of ALP, COL, and OSN on PS, TI, and AHS-TI (mean ± SD, n = 5). Note: On AHS-TI and TI, ALP and COL mRNA expression was down-regulated relative to that on PS at 3 and 4 wks. *$p < 0.05$. The expression levels of OSN mRNAs remained *quasi*-constant on the 3 materials throughout the culture period.

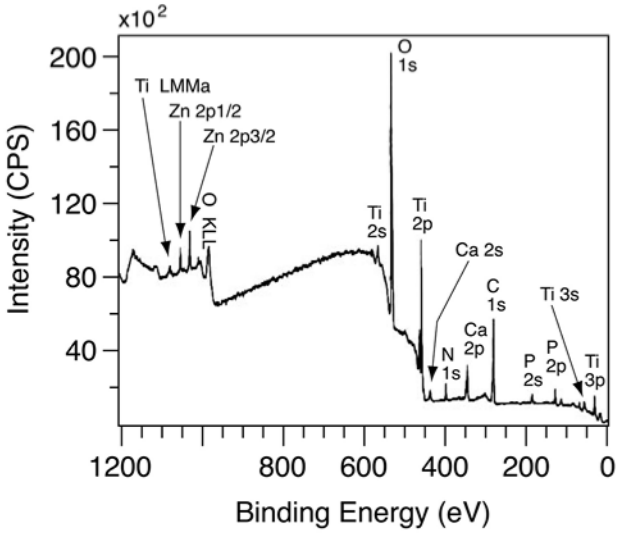

Figure 5. Immersion in α-MEM produced subtle Ca-P product on TI. XPS wide-scan spectra of the surface of polished titanium (TI) that had been immersed in α-MEM for 3 wks (n = 1). Note: Very subtle Ca-P products were noticed by identification of Ca 2s, Ca 2p, P 2s, and P 2p peaks.

(SBF), sodium titanate on AH-TI releases its Na^+ ions into the surrounding fluid *via* an exchange with the H_3O^+ ions in the fluid to form Ti-OH groups on its surface. These Ti-OH groups interact with calcium ions to form a calcium titanate. Negatively charged -OH groups on the surface effectively attract positively charged calcium ions. The calcium titanate incorporates phosphate ions in the fluid to induce apatite nucleation. Once the apatite nuclei are formed, they grow spontaneously by consuming calcium and phosphate ions contained in the SBF, because the fluid is already supersaturated with respect to the apatite. Impurities (*e.g.*, Mg, Cl, and HCO_3^-) are easily introduced in the formed apatite, constituting a composition analogous to that of natural bone mineral.

(4) The Expression Levels of ALP and COL mRNAs of Osteoblast-like SaOS-2 Cells on the 3 Materials Examined

On AHS-TI and TI, ALP and COL mRNA expression was down-regulated relative to that on PS at 3 and 4 wks ($p < 0.05$) (Fig. 4C). This means that AHS-TI and TI accelerated the osteogenic differentiation of SaOS-2. The expression levels of OSN mRNAs remained *quasi*-constant on the 3 materials throughout the culture period. The reason for this is not well-understood. OSN mRNAs might be constantly produced for purposes other than osteogenic differentiation.

(5) Effect of AHS-TI on the Osteogenic Differentiation of Osteoblastic-like SaOS-2 cells (further explanation)

It has been reported that the osteogenic differentiation of osteoblasts was accelerated on apatite compared with titanium or polystyrene culture dishes by examination of ALP activity and OSC production (Massas *et al.*, 1993; Massaro *et al.*, 2001). However, the expression of other osteogenic differentiation marker genes (mRNAs) of osteoblasts on apatite has not been well-studied (Hong *et al.*, 2003), while that of heterogeneous bone marrow stromal cells on apatite was not extensively examined either (Yoshikawa *et al.*, 1998). On AHS-TI, our results clarified that the expression of early-stage (ALP and COL) differentiation-related mRNAs was down-regulated and that of middle- to late-stage differentiation-related (OSP, BSP, and OSC) mRNAs tended to be up-regulated, in contrast to the results on PS and TI. Our studies confirm the induction and passage of osteogenic differentiation-related mRNAs on 3 materials, and we conclude that AHS-TI most accelerated the expression of osteogenic differentiation-related mRNAs, followed by TI, while PS least affected it.

(6) XPS of AH-TI Immersed in α-MEM for 3 Wks

Fig. 5 shows XPS wide-scan spectra of the surface of polished titanium (TI) that had been immersed in α-MEM for 3 wks. Some Ca-P products were observed on the surface. A similar situation was reported on titanium that had been kept in artificial body fluid (Hanks' solution) for a few wks (Hanawa and Ota, 1991). Ultra-thin Ca-P products on TI, not traceable with thin-film XRD, might accelerate the osteogenic differentiation of osteoblastic SaOS-2 cells, compared with the cells cultured on polystyrene dishes that lacked Ca-P products.

REFERENCES

Barrere F, van Blitterswijk CA, de Groot K, Layrolle P (2002). Nucleation of biomimetic Ca-P coatings on Ti6Al4V from a SBFx5 solution: influence of magnesium. *Biomaterials* 23:2211-2220.

Bigi A, Cojazzi G, Panzavolta S, Ripamonti A, Roveri N, Romanello M, *et al.* (1997). Chemical and structural characterization of the mineral phase from cortical and trabecular bone. *J Inorg Biochem* 68:45-51.

Han Y, Fu T, Lu J, Xu K (2001). Characterization and stability of hydroxyapatite coatings prepared by an electrodeposition and alkaline-treatment process. *J Biomed Mater Res* 54:96-101.

Hanawa T, Ota M (1991). Calcium phosphate naturally formed on titanium in electrolyte solution. *Biomaterials* 12:767-774.

Hong JY, Kim YJ, Lee HW, Lee WK, Ko JS, Kim HM (2003). Osteoblastic cell response to thin film of poorly crystalline calcium phosphate apatite formed at low temperatures. *Biomaterials* 24:2977-2984.

Jonasova L, Muller FA, Helebrant A, Strnad J, Greil P (2002). Hydroxyapatite formation on alkali-treated titanium with different content of Na^+ in the surface layer. *Biomaterials* 23:3095-3101.

Lee BH, Do Kim Y, Shin JH, Hwan Lee K (2002). Surface modification by alkali and heat treatments in titanium alloys. *J Biomed Mater Res* 61:466-473.

Massaro C, Baker MA, Cosentino F, Ramires PA, Klose S, Milella E (2001). Surface and biological evaluation of hydroxyapatite-based coatings on titanium deposited by different techniques. *J Biomed Mater Res (Appl Biomater)* 58:651-657.

Massas R, Pitaru S, Weinreb MM (1993). The effects of titanium and hydroxyapatite on osteoblastic expression and proliferation in rat parietal bone cultures. *J Dent Res* 72:1005-1008.

Takadama H, Kim HM, Kokubo T, Nakamura T (2001). An x-ray photoelectron spectroscopy study of the process of apatite formation on bioactive titanium metal. *J Biomed Mater Res* 55:185-193.

van Dijk K, Schaeken HG, Wolke JG, Jansen JA (1996). Influence of annealing temperature on RF magnetron sputtered calcium phosphate coatings. *Biomaterials* 17:405-410.

Yoshikawa T, Ohgushi H, Akahane M, Tamai S, Ichijima K (1998). Analysis of gene expression in osteogenic cultured marrow/hydroxyapatite construct implanted at ectopic sites: a comparison with the osteogenic ability of cancellous bone. *J Biomed Mater Res* 41:568-573.